

pubs.acs.org/est Article

Tandem Fluorescence Measurements of Organic Matter and Bacteria Released in Sea Spray Aerosols

Mitchell V. Santander, Brock A. Mitts, Matthew A. Pendergraft, Julie Dinasquet, Christopher Lee, Alexia N. Moore, Lucia B. Cancelada, Ke'La A. Kimble, Francesca Malfatti, and Kimberly A. Prather*



Cite This: Environ. Sci. Technol. 2021, 55, 5171-5179



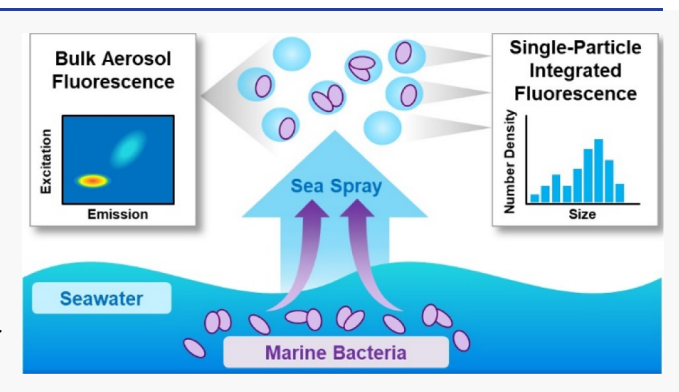
ACCESS

III Metrics & More

Article Recommendations

s Supporting Information

ABSTRACT: Biological aerosols, typically identified through their fluorescence properties, strongly influence clouds and climate. Sea spray aerosol (SSA) particles are a major source of biological aerosols, but detection in the atmosphere is challenging due to potential interference from other sources. Here, the fluorescence signature of isolated SSA, produced using laboratory-based aerosol generation methods, was analyzed and compared with two commonly used fluorescence techniques: excitation—emission matrix spectroscopy (EEMS) and the wideband integrated bioaerosol sensor (WIBS). A range of dynamic biological ocean scenarios were tested to compare EEMS and WIBS analyses of SSA. Both techniques revealed similar trends in SSA fluorescence intensity in response to changes in ocean microbiology,



demonstrating the potential to use the WIBS to measure fluorescent aerosols alongside EEMS bulk solution measurements. Together, these instruments revealed a unique fluorescence signature of isolated, nascent SSA and, for the first time, a size-segregated emission of fluorescent species in SSA. Additionally, the fluorescence signature of aerosolized marine bacterial isolates was characterized and showed similar fluorescence peaks to those of SSA, suggesting that bacteria are a contributor to SSA fluorescence. Through investigation of isolated SSA, this study provides a reference for future identification of marine biological aerosols in a complex atmosphere.

1. INTRODUCTION

Biological aerosols, or bioaerosols, are particles that include organisms, biological fragments, excretions, or dispersal units. These particles are ubiquitous in the atmosphere and can have profound effects on clouds and climate by acting as cloud condensation nuclei and ice nuclei in clouds. Therefore, there is a strong interest to identify bioaerosols and understand their atmospheric dynamics. A widely used method for bioaerosol identification is fluorescence spectroscopy, which exploits the intrinsically fluorescent biomolecules found in these aerosols. However, aerosols in the atmosphere are often externally mixed populations from different sources, making it a challenge to separate particle types based on fluorescence alone. Thus, it is necessary to characterize the fluorescence of isolated particle sources to disentangle the impact of different bioaerosols in the atmosphere.

The oceans have been shown to be a major source of bioaerosols, *via* sea spray aerosol (SSA) particles.^{1,3} SSA particles are produced when bubbles, entrained by breaking waves, burst at the sea surface. SSA composition can vary depending on the biological state of the ocean.^{4–6} Previous studies have shown that SSA particles contain bacteria, cell fragments, viruses, enzymes, and other biomolecules that can

influence the climate and relevant cloud properties.^{7,8} Despite the potential for marine bioaerosols to play a major role in climate, very few studies have used fluorescence as a tool to identify bioaerosols released during nascent SSA production.^{9–12} This is, in part, due to the difficulty of using fluorescence to study SSA in the real atmosphere without a basic understanding of the fluorescence signature of SSA.

Here, the fluorescence characterization for isolated, laboratory-generated SSA is reported. Two common fluorescence methods were used to characterize SSA: excitation—emission matrix spectroscopy (EEMS) and a wideband integrated bioaerosol sensor (WIBS). EEMS has been widely used to characterize organic matter in a variety of aqueous environments, including seawater. EEMS has the advantage of taking direct, full-spectrum fluorescence measurements of aqueous samples and can be used to investigate offline, bulk

Received: August 14, 2020 Revised: January 7, 2021 Accepted: January 8, 2021 Published: March 23, 2021





Table 1. Layout of the Three Experimental Setups Used in This Study

Experiment number	Bulk solution	Additions	Aerosol generation	Fluorescence measurements
Experiment 1	seawater	none	wave channel	EEMS bulk solution, EEMS aerosol, and WIBS aerosol
Experiment 2	seawater	F/100 nutrients ^a , sodium silicate	MART	EEMS bulk solution, EEMS aerosol, and WIBS aerosol
Experiment 3a	seawater and filtered, autoclaved seawater	F/2 nutrients ^a	miniMART	EEMS bulk solution and WIBS aerosol
Experiment 3b	4× PBS with bacterial isolates	none	miniMART	EEMS bulk solution and WIBS aerosol

[&]quot;Final concentration of Guillard's growth medium. A final concentration of F/2 is defined by Guillard & Ryther (1962), therefore, a concentration of F/100 is a 50× dilution.

aerosol chemistry. The WIBS collects online, single-particle fluorescence measurements at lower resolution and has been increasingly used to investigate the dynamics of atmospheric bioaerosols in both the laboratory and the field. 10,15-18 However, no studies have used the WIBS to directly measure isolated, nascent SSA in a laboratory setting. In the present study, single-particle and bulk aerosol fluorescence were used to evaluate realistic SSA and determine how SSA fluorescence changes under dynamic ocean biological conditions (e.g., during a phytoplankton bloom). Additionally, these techniques were used to characterize the contribution of marine bacteria to SSA fluorescence through controlled experiments involving isolated marine bacteria and abiotic seawater. This study provides a framework for using a fluorescence approach to investigate how temporal changes in biological species affect SSA released into the environment.

2. METHODS

2.1. Aerosol Generation and Experiment Design. SSA particles were generated using three different methods: a wave channel located at the Scripps Institution of Oceanography, 4,5 a Marine Aerosol Reference Tank (MART), 19,20 or a miniature Marine Aerosol Reference Tank (miniMART).²¹ Each of these aerosol generation methods are isolated systems, without the influence of non-biological fluorescent particles from terrestrial or anthropogenic sources. Additionally, each of these methods produces aerosol size distributions and chemical compositions which mimic that of a breaking ocean wave. 21,22 The three experimental methods also differed in biological activity in the seawater: (1) seawater without a phytoplankton bloom; (2) seawater with Guillard's nutrient medium added to generate a phytoplankton bloom with natural marine microbial communities;²³ and (3) control scenarios consisting of either abiotic seawater or cultured marine bacterial strains in a phosphatebuffered saline solution (4× PBS). Details of the three experiments are provided in Table 1 and Supporting Information.

2.2. Aerosol and Seawater Sample Collection. Aerosol samples were measured in real time with the WIBS and collected into a liquid solution for EEMS measurements. Prior to detection with the WIBS, aerosols were dried using inline silica diffusion driers to maintain a relative humidity of <20% throughout all experiments. As a result of drying and partial quenching of the fluorophores, it is possible that a fraction of fluorescent particles was below the fluorescence threshold. While channel 1 may not be affected due to the strong emission of tryptophan, humic-like substances (HULIS) can show decreased emission when in a powder state. ²⁴ However, SSA particles have been shown to be semisolid below the

efflorescence point,²⁵ therefore, drying should not have a significant effect on the observed trends.

For EEMS analysis of the bulk aerosol, collection involved a liquid spot sampler (Aerosol Devices Inc., 110A), which uses a water condensation growth tube to collect particles directly into a liquid medium with high efficiency. Aerosols passing through the spot sampler were collected in ultrapure water. Although collection into ultrapure water could potentially change the fluorescence intensity due to bacterial lysis and subsequent solvent exposure, these changes would be slight, due to the lack of new tryptophan formation/breakdown. Additionally, any changes would be consistent throughout the course of these experiments. SSA particles were collected for experiments 1 and 2 at a flow rate of 1.5 liters per minute (LPM) for 1 h on the MART or overnight (12 h) on the wave channel. No aerosols were collected for EEMS analysis for experiment 3 (miniMART).

Seawater collection for EEMS analysis was performed for each experiment. For all experiments, seawater samples were collected into either 15 or 50 mL sterile, polypropylene tubes. Seawater samples were collected during aerosol generation for experiment 2 and either prior to, or immediately after, aerosol generation for the other experiments. Excitation—emission matrices (EEMs) were generally measured within 20 min of collection.

2.3. Bacterial Isolate Culture Preparation. Three different marine-relevant bacterial isolates were chosen due to their presence in the coastal waters off of Scripps Pier: AltSIO, ATW7, and BBFL7. 27,28 All isolates were originally derived from the Pacific Ocean off the Scripps Pier in La Jolla, California and isolated by the Azam laboratory at the Scripps Institution of Oceanography. For this experiment, bacterial isolates were streaked out from a frozen glycerol stock onto ZoBell medium. After 24 h, colonies were picked and grown in liquid ZoBell medium at room temperature on a shaker (130 rpm). The next day, the cultures were harvested through 5 min of centrifugation at 9000g and washed with PBS to remove the supernatant (spent medium). Optical density was measured at 600 nm in order to have a 1:1:1 (AltSIO/ATW7/BBFL7) ratio of the three cultures in the inoculum with a concentration of 1 \times 10⁹ cells/mL. The final concentration of bacterial cells in the miniMART was $\sim 1.6 \times 10^5$ cells/mL, which is on the order of known bacterial concentrations in the ocean, especially in oligotrophic regions.29

2.4. Fluorescence Measurements. 2.4.1. WIBS. Online, single-particle fluorescence measurements were taken using a WIBS (Droplet Measurement Technologies, WIBS-NEO). The WIBS operation has been described previously in detail. ¹⁵ Briefly, the WIBS utilizes two xenon lamps with bandpass filters to generate two excitation wavelengths at 280 nm (Xe1)

and 370 nm (Xe2). These excitation wavelengths are intended to target the fluorescence excitation of the amino acid tryptophan and the biological cofactor nicotinamide adenine dinucleotide (NADH), respectively.³⁰ The WIBS collects the fluorescence emission from a particle using two photomultiplier tubes (PMTs) with bandpass filters from 310 to 400 nm (FL1) and from 420 to 650 nm (FL2). This arrangement creates three main combinations of fluorescence excitation and emission "channels," with different target molecules. These channels are labeled here as channel 1 (Xe1/FL1; Ex/Em = 280 nm/310-400 nm; targeting tryptophan), channel 2 (Xe1/FL2; 280 nm/420-650 nm; targeting riboflavin), and channel 3 (Xe2/FL2; 370 nm/420-650 nm, targeting NADH). We focus primarily on channels 1 and 3 as these channels coincide with the EEM peaks representing the fluorescence from protein-like and HULIS, respectively. Additionally, we exclude channel 2 from most of our discussion due to the potential cross-sensitivity of this channel with the other two channels, as reported previ-

A forced trigger sampling period, where the sample flow is off and the xenon lamps are fired, was performed at the start of each day to provide a blank for the fluorescent particle detection. Particles are deemed fluorescent if they exceed a minimum threshold

$$E_{\text{Threshold}_i} = 3\sigma_i + \overline{E}_i \tag{1}$$

where \overline{E}_i is the mean background fluorescence from the forced trigger data and σ_i is the standard deviation of the background for each fluorescence channel (FL_i), as described in previous studies. The fluorescence values for particles detected by the WIBS were then subtracted by the forced trigger thresholds for each individual channel. The WIBS-NEO has greater dynamic range compared to previous models, which prevents saturation of the detector for highly fluorescent particles. The intensity values reported are in arbitrary units; however, the mean SSA intensity values were converted to mass equivalents of tryptophan (channel 1) and quinine (channel 2 and 3) based on a similar calibration to that defined by Robinson *et al.* (2017) (Supporting Information, Figure S1).

The WIBS uses a 635 nm continuous-wave laser to detect, size, and determine the shape of single particles. Optical diameter measurements, from 0.5 to 50 μ m, are based on detection of side-scattered light with the FL2 PMT. Analysis of forward-scattered light on a quadrant PMT determines the asymmetry factor (AF) for each particle. The AF is a measure of the shape of a particle, with an AF <10-15 indicative of nearly spherical particles, an AF of 15-30 for aspherical particles, and an AF >30 for rod- or fiber-shaped particles. 16,34 The single-particle optical diameter, measured with the WIBS, was used to calculate the size distribution of fluorescent particles in each channel. Polystyrene latex spheres were used to verify the accuracy of the WIBS optical diameter measurements. For the size distribution measurements, size bins were divided into 32 bins per decade of optical diameter. Particle counts are displayed as the number concentration of fluorescent particles per liter of air divided by the logarithm of the bin width $(dN/d\log D_p)$. In addition to the forced trigger fluorescence threshold, a size threshold was applied to all particles measured with the WIBS. Particles with optical diameters less than $D_p = 0.8 \mu m$ were excluded from these analyses because of previously reported inaccuracies in the fluorescence detector sensitivity and counting efficiency of smaller particles. 16,31 For bacterial isolate size distributions, a fluorescence cutoff of 2.5 standard deviations above the mean background PBS fluorescence in channel 1 was applied to eliminate most PBS particles.

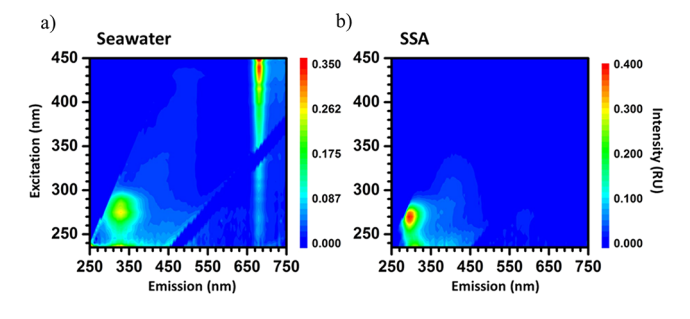
2.4.2. EEMS. Offline, bulk fluorescence EEMs of seawater and SSA collected with the liquid spot sampler were measured with an Aqualog spectrophotometer (HORIBA Scientific, extended range). Collection periods of at least 1 h on a MART at 1.5 LPM or approximately 12 h at 1.5 LPM on the wave channel were used to obtain an adequate fluorescence signal from the protein-like region and often sufficient signal for the HULIS region, depending on seawater biology and chemistry. No processing of seawater samples was necessary to acquire fluorescence signals. Excitation wavelengths ranged from 230 to 500 nm, while the emission collection bands ranged from 250 to 800 nm, both in ~5 nm increments. Background spectra acquired using ultrapure water or PBS solution were subtracted from all EEMs. EEMs were then corrected for inner filter effects based on the absorbance spectra measured simultaneously. Rayleigh scattering (1st and 2nd order) was removed from all spectra. EEMs were normalized to the area of the Raman scattering peak of water at 350 nm excitation to convert fluorescence intensities to Raman Units. 35,36 A comparison between the EEM spectrum and the WIBS channels is highlighted in Figure S2.

3. RESULTS

Three different experiments, with varying biological complexity and activity, were studied in order to compare the fluorescence measurements of EEMS and the WIBS. Experiment 1 used a wave channel and fresh seawater to replicate SSA production of the natural microbial community in coastal seawater with low phytoplankton biomass. Experiment 2 involved a MART for aerosolization of seawater induced with a phytoplankton bloom, typical of realistic bloom conditions with high biomass. Experiment 3 was used as a control of two different scenarios involving a miniMART: abiotic seawater and a pure bacterial system in a salt solution.

3.1. Experiment 1: Bulk Aerosol and Single-Particle Fluorescence of Nascent SSA. EEMs for seawater showed fluorescence in regions that are commonly detected for marine systems (Figure 1a). 12,37 Specifically, three fluorescence regions were present, representing three different classes of organic molecules. Fluorescence in the region at excitation/ emission wavelengths 400-440 nm/680-690 nm is indicative of chlorophyll a. 12 Fluorescence at excitation/emission wavelengths <235 nm and 275-280 nm/330-350 nm is attributed to protein-like substances and typically indicates fluorescence from the amino acid tryptophan. In this study, the 275-280 nm excitation was used as an indicator for protein-like fluorescence because of the excitation bounds of the EEMs. Components that emit in this region range from bacteria cells to viruses to proteinaceous gels. 12,38,39 EEM features near 260 nm or 360 nm/450-455 nm and at 325 nm/410 nm are indicative of HULIS, complex mixtures of organic molecules produced during the breakdown of organisms and larger biomolecules. 12,37,40

EEMs for SSA collected from the wave channel showed different fluorescence signatures than those in seawater, indicating chemical species are selectively transferred into SSA (Figure 1b). In contrast to seawater, SSA EEMs did not show chlorophyll *a* signatures, suggesting that larger phytoplankton species are not efficiently transferred. While



(c)	Channel 1	Channel 2	Channel 3
	(280 nm/310-400 nm)	(280 nm/420-650 nm)	(370 nm/420-650 nm)
Intensity (a.u.)	1.245e5 ± 5.368e5	$2.491e4 \pm 6.560e4$	$3.608e4 \pm 1.045e5$
Diameter (µm)	2.19 ± 1.01	2.03 ± 0.93	1.63 ± 0.82
AF (a.u.)	6.23 ± 3.25	6.10 ± 3.14	5.57 ± 2.79

Figure 1. Selected EEMs for (a) seawater and (b) nascent SSA collected from the wave channel. (c) WIBS measurements of the mean fluorescence intensity, optical diameter, and AF for each fluorescence channel (excitation/emission) for SSA generated by the wave channel.

both seawater and SSA EEMs showed protein-like and humiclike signatures, SSA EEMs were primarily dominated by protein-like fluorescence with a smaller contribution from HULIS. The ratio of the protein-like peak (Ex: 275 nm/Em: 330 nm) to the humic-like peak (Ex: 360 nm/Em: 450 nm) was evaluated for both samples. The protein-to-humic intensity ratio for seawater was 12.87, whereas the ratio for SSA was 15.63, confirming the increased contribution of protein-like fluorescence in SSA. Additionally, the SSA EEMs showed a shift in the protein-like emission spectra when compared to the protein-like fluorescence in seawater. While seawater showed fluorescence primarily from tryptophan, with an emission peak close to 350 nm, SSA EEMs showed a major peak in the emission spectra closer to 300 nm, indicative of fluorescence from the amino acid tyrosine. Tyrosine fluorescence suggests the presence of marine gels or exopolymeric substances in SSA. 41 The tyrosine peak lies outside the range of wavelengths detected by the WIBS (310-400 nm), thus some portion of SSA fluorescence was not captured using this analytical method. However, the protein peak in SSA extended to longer wavelengths, suggesting that tryptophan fluorescence was also present and therefore detectable with the WIBS.

Across 7 days of sampling nascent SSA particles generated from the wave channel, the WIBS measured over 100,000 individual fluorescent particles each day. The fluorescent fraction in this low biomass scenario represented $0.87 \pm 0.09\%$ of all particles measured with optical diameters greater than D_n = 0.8 μ m. The fluorescent fraction measured was relatively low compared to ambient measurements which range from 1.9% to upward of 40% but are often influenced by terrestrial bioaerosols. 16,42 In order to define a distinct fluorescence signature for isolated SSA, mean fluorescence intensities of the different fluorescence channels were calculated from all sampling days combined (Figure 1c). Additionally, the channel-specific mean AF and diameter were calculated for fluorescent SSA particles. Particles across all three channels had low AF (\sim 6), with channel 3 particles showing the lowest AF. These low AFs demonstrate that most of the fluorescent particles detected were spherical or spheroidal in shape. The mean diameter of SSA measured in channel 1 was, in general, larger than those in channel 3, indicating different chemical species are transferred into different particle sizes.

The mean daily size distributions of SSA particles generated by the wave channel were measured with the WIBS and separated based on the fluorescence channels (Figure 2). The

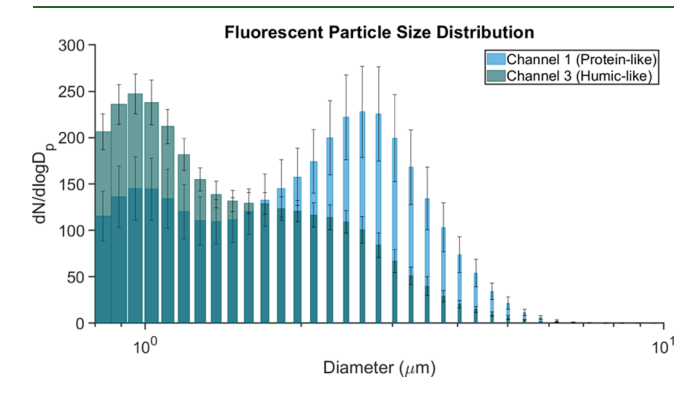


Figure 2. SSA size distributions separated by fluorescence channels measured with the WIBS. Channel 1 (protein-like) is in blue with channel 3 (humic-like) overlaid in green. Both size distributions shown are the daily mean particle counts (#/L) normalized to the bin widths, and the error bars represent one standard deviation from the mean.

size distributions measured with the WIBS showed a bimodal distribution for channel 1, with a peak optical diameter around $D_p = 2.6 \ \mu \text{m}$ and a second mode near $D_p = 1 \ \mu \text{m}$. The largersized mode is suggestive of proteinaceous molecules ejected in supermicron-sized aerosols. Bacteria, which contain a high protein content, have been observed in coarse mode aerosols measured in nascent SSA and off coastal regions. 43,44 Previous WIBS studies show that bacteria have dominant fluorescence emission in channel 1 due to the amino acid tryptophan. 17,18 Additionally, a fraction of particles that fluoresced in channel 1 also fluoresced in channel 3 (ca. 7% of all channel 1 particles). The particles that fluoresced in both channels 1 and 3 showed a size distribution resembling the main mode for channel 1 fluorescent particles, slightly shifted to larger sizes (Figure S3). The size distribution and fluorescence signature of the particles that fluoresced in both channels 1 and 3 suggest that these particles may be metabolically active bacteria, with enhanced NADH. Furthermore, bacteria bound to gels and transparent exopolymeric particles have been observed in this size range. 45,46 Bound bacteria are often larger and enzymatically active which may explain the shift to larger sizes for particles that fluoresce in both channels 1 and 3.

For particles fluorescing in the WIBS channel 3, a peak in the size distribution was observed near $D_p = 1 \mu m$ with a tail extending into the larger sizes (Figure 2). In an ambient setting, fluorescence in this channel is often associated with pollen and fungal spores. However, in this study of isolated, nascent SSA, fluorescence in this channel was likely indicative of HULIS, as shown in previous work by Savage et al. (2017).¹⁷ Measurements on the molecular weight of marinebased HULIS show that it typically consists of small molecules, with 90% of the measured HULIS mass falling below 5 kDa. HULIS, by nature, is part of dissolved organic matter in the ocean and is therefore expected to be released across particles of all sizes.⁴⁹ The shape of the total particle size distribution (combined fluorescent and non-fluorescent), measured for SSA generated by the wave channel, was similar to that of channel 3 (Figure S4). This similarity further suggests that the

channel 3 measurements by the WIBS are indicative of dissolved HULIS in SSA.

3.2. Experiment 2: Changes in Fluorescence Signatures During a Phytoplankton Bloom. SSA fluorescence was measured with both the WIBS and EEMS throughout an induced phytoplankton bloom to investigate the effect of a changing marine biological state on SSA. The microbial dynamics were measured throughout the course of the phytoplankton bloom (Figure S5). The experiment occurred over 9 days with *in vivo* chlorophyll *a* fluorescence indicating a peak in phytoplankton growth on the third day, followed by senescence for the remainder of the experiment. Heterotrophic bacteria concentrations peaked on the fifth day and declined afterward. Virus concentrations tracked the heterotrophic bacteria concentrations and increased after the peak in the phytoplankton bloom (Figure S5).

WIBS measurements of the SSA fluorescence intensity corresponded with SSA EEMs throughout the phytoplankton bloom (Figure 3). WIBS channel 1 (protein-like) showed a

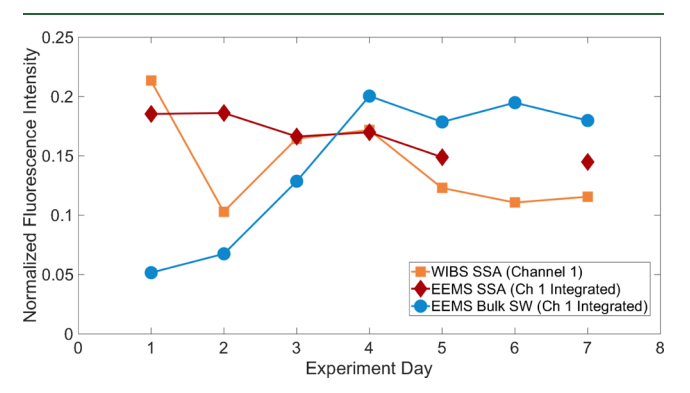


Figure 3. WIBS fluorescence channel 1 (protein-like) graphed over time during a phytoplankton bloom. EEM emission integrated over the same wavelengths measured by the WIBS shown over time for both bulk seawater (bulk SW) and SSA over the course of a phytoplankton bloom. All values are normalized to the sum of intensities for each measurement across all the days of the experiment.

general decrease in fluorescence intensity over time. The decreasing fluorescence trend was also observed for the SSA EEMs upon integrating over the same wavelengths of WIBS channel 1. The trends in WIBS channel 1 and EEM proteinlike region revealed a disconnect between the fluorescence observed in SSA and the fluorescence in seawater over the course of the bloom (Figure 3). However, when the WIBS channel 3 measurements were compared to the corresponding seawater HULIS-region fluorescence measured with EEMS, the SSA mean fluorescence intensity generally agreed with that in the seawater (Figure S6). The difference in enrichment for HULIS and protein-like species into the aerosol indicates a chemical-specific transfer. More studies are required to determine which factors affect the selective transfer of fluorescent species from seawater to SSA. Nevertheless, the similarity between the WIBS and EEMS measurements of SSA over time reveals that single-particle fluorescence, in combination with seawater analysis, can provide unique insights on SSA composition throughout a wide range of ocean biological conditions.

3.3. Experiment **3:** Characterizing the Fluorescence of Abiotic Seawater and Bacterial Isolates. In order to probe the contribution of marine bacteria to SSA fluorescence, the WIBS and EEMS were used to measure fluorescence under

two controlled scenarios: (1) natural seawater *vs* filtered, autoclaved seawater (FASW) and (2) marine bacterial isolates in a salt solution. As mentioned previously, seawater used for the FASW experiment was taken from a separate phytoplankton bloom experiment and the bacterial isolate experiment was run with a PBS medium to minimize background fluorescence.

To better understand the underlying fluorescence signature of SSA, changes in both seawater and SSA fluorescence were measured with EEMS and the WIBS before and after sterilization of the seawater. The FASW EEMs showed an increase in the humic-like fluorescence intensity compared to natural seawater EEMs, suggesting an enhanced production of HULIS during the autoclaving process (Figure 4a).⁵⁰ The enhanced production of HULIS or a potential change in the selectivity, leading to aerosol enrichment, might explain the increase in the WIBS channel 3 size distribution for FASW SSA (Figure 4b). Additionally, WIBS measurements on FASW SSA showed a decrease in the $D_p = 2-3 \mu m$ sized mode in the channel 1 fluorescence size distribution compared to natural SSA (Figure 4d), suggesting a lack of large, protein-containing particulates in FASW SSA. The decrease in the WIBS channel 1 size distribution was not as significant as the diminishment in the EEM protein-like feature (Figure 4c), likely because the fluorescent material (reduced but still detected by EEMS) was detected by the WIBS and contributed to the fluorescence size distribution. However, the trends of both instruments further suggest that marine microbes are contributing to the large size mode observed in the WIBS channel 1 size distribution measured for SSA.

To further elucidate the contribution of marine bacteria to SSA fluorescence, the bulk and aerosol fluorescence signatures were characterized for a solution containing three marine bacterial isolates (AltSIO, ATW7, and BBFL7) (Figure 5). The bacterial EEMs showed high fluorescence in the protein region, with no noticeable humic-like fluorescence above the background 4× PBS (Figure 5a). This spectrum shared similar characteristics to previously measured EEMs of marine bacteria.³⁸ The three individual bacteria were also analyzed separately using EEMS and showed similar spectra with fluorescence predominantly in the protein region and negligible fluorescence in the HULIS region (Figure S7). This result indicates that the fluorescence signature of the marine bacterial solution containing all three bacteria was not dominated by one species. The tryptophan-like fluorescence regions from marine bacterial EEMs were also present in seawater and SSA EEMs, suggesting that bacteria are a component in SSA fluorescence.

The WIBS fluorescence measurements of the bacteria aerosolized with a miniMART showed similar signatures to those detected by EEMS. The bacterial isolates showed an increased mean fluorescence intensity in channel 1 compared to the 4× PBS medium (Figure S8). These results were similar to previous WIBS studies, which found that terrestrial bacterial cultures fluoresce strongly in channel 1. Moreover, the increase in mean fluorescence intensity was not seen in the other two channels measured by the WIBS. The WIBS fluorescence signature for aerosolized marine bacteria paralleled the EEMs of the bacteria in solution, further highlighting the capability of single-particle fluorescence for SSA characterization.

WIBS channel 1 size distribution for the aerosolized bacterial isolates was generated in the same manner to those generated for the wave channel. The background-corrected,

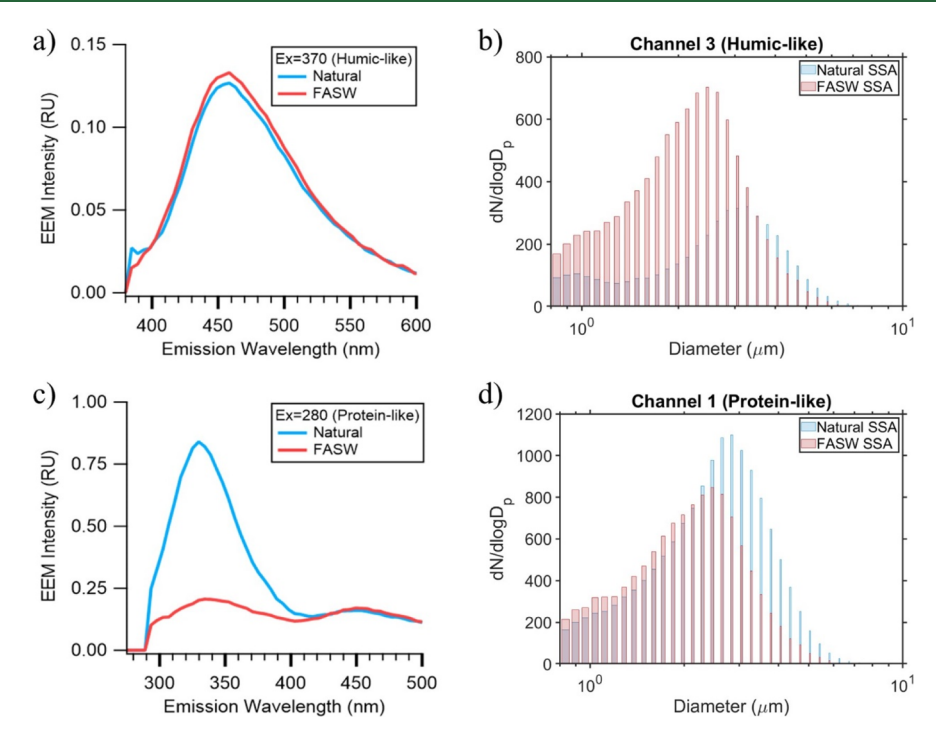


Figure 4. Emission spectra from the EEMs of the natural seawater and FASW corresponding to the excitation wavelengths for (a) WIBS channel 3 and (c) WIBS channel 1. Fluorescence size distributions of SSA before and after filtering and autoclaving for (b) WIBS channel 3 and (d) WIBS channel 1.

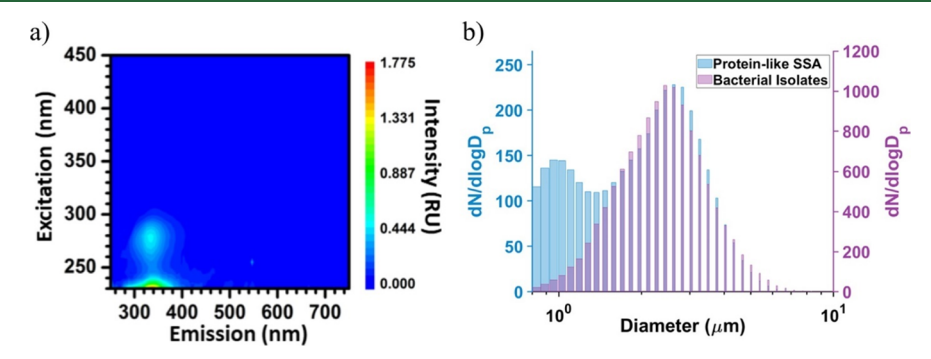


Figure 5. Fluorescence of the bacterial isolate mixture measured by (a) EEMS (adjusted to the blank EEM of the 4× PBS solution). (b) WIBS channel 1 fluorescence size distribution of the bacterial isolates that fluoresced above the PBS background (purple), overlaid on the mean channel 1 size distribution of the wave channel SSA (blue).

fluorescent particle size distribution showed that the bacterial isolates were ejected into predominantly larger particles with the peak of the distribution near $D_p = 2.4 \mu m$ (Figure 5b). The mode of the size distribution for the bacterial isolates was resemblant of the protein-like, nascent SSA measured from the wave channel, indicating that the particles detected in the wave channel likely included bacteria (Figure 5b). Slight differences in the size distributions between the seawater and the bacterial isolates might be explained by the proteinaceous constituents in chemically complex seawater compared to the 4× PBS and the formation of proteinaceous aggregates in natural SSA.⁴⁶ While further work is necessary to fully elucidate the contribution of marine bacteria in SSA and their transport pathways, it is clear that marine bacteria can be ejected into the atmosphere via SSA particles and detected using fluorescence techniques.

3.4. Implications. When evaluating which fluorescence technique is appropriate for a specific measurement, multiple factors should be considered. Due to the additional steps

necessary in measuring SSA using EEMS, such as impinging the aerosols into a bulk medium, this instrument is better suited for measurements of bulk seawater. However, the WIBS is a useful instrument for characterizing real-time changes in single-particle SSA and shows comparable trends to fluorescence measured with EEMS. Therefore, WIBS aerosol measurements, in tandem with EEMS analysis of bulk solutions, can provide a thorough investigation of fluorescent particle production. Possible modifications to the optics of the WIBS for improved characterization of SSA may involve extending the fluorescence emission collection of channel 1 to include the major peak of tyrosine fluorescence, shown to be significant in the SSA EEMs.

SSA particles represent one of the most abundant natural aerosols in the atmosphere, ⁵¹ but only during the past decade have their role as primary biological aerosols been a major focus of investigation. The unique ability of bioaerosols to affect clouds and climate becomes especially important in remote marine locations where SSA particles can dominate as

cloud condensation nuclei or ice nuclei.^{1,52–54} With growing interest in the atmospheric dynamics of bioaerosols, uncovering the role of SSA has become increasingly critical to our understanding of how bioaerosols influence climate. Our investigations on isolated systems provide a basis for the fluorescence signature of SSA to help unravel the complex trends observed in the atmosphere and move toward identification of marine bioaerosols in the natural environment.

ASSOCIATED CONTENT

Supporting Information

The Supporting Information is available free of charge at https://pubs.acs.org/doi/10.1021/acs.est.0c05493.

Descriptions of the three experiments and methods on microbial enumeration; WIBS channel calibration and conversion to equivalent fluorophore mass; overlap of the WIBS channels with the EEM spectrum; size distribution for particles in channels 1, 3, and 1 and 3; size distribution of the total and humic-like particles; microbial activity for the phytoplankton bloom experiment; trends in the WIBS and EEMs for humic-like fluorescence; EEMs for the individual bacterial isolates; and the mean intensity for the bacterial isolates measured with the WIBS (PDF)

AUTHOR INFORMATION

Corresponding Author

Kimberly A. Prather — Department of Chemistry and Biochemistry, University of California San Diego, La Jolla, California 92093, United States; Scripps Institution of Oceanography, University of California San Diego, La Jolla, California 92037, United States; Email: kprather@ucsd.edu

Authors

Mitchell V. Santander – Department of Chemistry and Biochemistry, University of California San Diego, La Jolla, California 92093, United States

Brock A. Mitts – Department of Chemistry and Biochemistry, University of California San Diego, La Jolla, California 92093, United States; orcid.org/0000-0001-5936-8748

Matthew A. Pendergraft — Scripps Institution of Oceanography, University of California San Diego, La Jolla, California 92037, United States; ◎ orcid.org/0000-0003-4415-7651

Julie Dinasquet – Scripps Institution of Oceanography, University of California San Diego, La Jolla, California 92037, United States

Christopher Lee – Scripps Institution of Oceanography, University of California San Diego, La Jolla, California 92037, United States

Alexia N. Moore – Department of Chemistry and Biochemistry, University of California San Diego, La Jolla, California 92093, United States

Lucia B. Cancelada – Department of Chemistry and Biochemistry, University of California San Diego, La Jolla, California 92093, United States

Ke'La A. Kimble — Department of Chemistry and Biochemistry, University of California San Diego, La Jolla, California 92093, United States

Francesca Malfatti – University of Trieste^{RINGGOLD}, Trieste 34140, Italy; Scripps Institution of Oceanography, University

of California San Diego, La Jolla, California 92037, United States; oorcid.org/0000-0002-0957-9288

Complete contact information is available at: https://pubs.acs.org/10.1021/acs.est.0c05493

Author Contributions

M.V.S. and B.A.M. contributed equally to the writing of this manuscript. The manuscript was written through contributions of all authors. All authors have given approval to the final version of the manuscript.

Notes

The authors declare no competing financial interest. All data supporting the conclusions are publicly available at: https://doi.org/10.6075/JOXK8D31.

ACKNOWLEDGMENTS

The authors would like to thank the National Science Foundation Center for Aerosol Impacts on the Chemistry of the Environment (NSF CAICE), a Center for Chemical Innovation (CHE-1801971) for funding this project. We thank Kathryn J. Mayer and Michael R. Alves for their thoughtful contributions and edits to this manuscript. We also thank the anonymous reviewers for their helpful comments and advice.

ABBREVIATIONS

AF asymmetry factor

EEMS excitation—emission matrix spectroscopy

EEM excitation—emission matrix FASW filtered, autoclaved seawater HULIS humic-like substance

LPM iters per minute

MART marine aerosol reference tank

miniMART miniature marine aerosol reference tank NADH nicotinamide adenine dinucleotide

PMT photomultiplier tube

PBS phosphate-buffered saline solution

SSA sea spray aerosol

SW seawater

WIBS wideband integrated bioaerosol sensor

■ REFERENCES

- (1) Fröhlich-Nowoisky, J.; Kampf, C. J.; Weber, B.; Huffman, J. A.; Pöhlker, C.; Andreae, M. O.; Lang-Yona, N.; Burrows, S. M.; Gunthe, S. S.; Elbert, W.; Su, H.; Hoor, P.; Thines, E.; Hoffmann, T.; Després, V. R.; Pöschl, U. Bioaerosols in the Earth System: Climate, Health, and Ecosystem Interactions. *Atmos. Res.* **2016**, *182*, 346–376.
- (2) Pöhlker, C.; Huffman, J. A.; Pöschl, U. Autofluorescence of Atmospheric Bioaerosols Fluorescent Biomolecules and Potential Interferences. *Atmos. Meas. Tech.* **2012**, *5*, 37–71.
- (3) Després, V. R.; Alex Huffman, J.; Burrows, S. M.; Hoose, C.; Safatov, A. S.; Buryak, G.; Fröhlich-Nowoisky, J.; Elbert, W.; Andreae, M. O.; Pöschl, U.; Jaenicke, R. Primary Biological Aerosol Particles in the Atmosphere: A Review. *Tellus, Ser. B: Chem. Phys. Meteorol.* **2012**, *64*, 15598.
- (4) Wang, X.; Sultana, C. M.; Trueblood, J.; Hill, T. C. J.; Malfatti, F.; Lee, C.; Laskina, O.; Moore, K. A.; Beall, C. M.; McCluskey, C. S.; Cornwell, G. C.; Zhou, Y.; Cox, J. L.; Pendergraft, M. A.; Santander, M. V.; Bertram, T. H.; Cappa, C. D.; Azam, F.; DeMott, P. J.; Grassian, V. H.; Prather, K. A. Microbial Control of Sea Spray Aerosol Composition: A Tale of Two Blooms. ACS Cent. Sci. 2015, 1, 124–131
- (5) Prather, K. A.; Bertram, T. H.; Grassian, V. H.; Deane, G. B.; Stokes, M. D.; DeMott, P. J.; Aluwihare, L. I.; Palenik, B. P.; Azam, F.; Seinfeld, J. H.; Moffet, R. C.; Molina, M. J.; Cappa, C. D.; Geiger, F.

- M.; Roberts, G. C.; Russell, L. M.; Ault, A. P.; Baltrusaitis, J.; Collins, D. B.; Corrigan, C. E.; Cuadra-Rodriguez, L. A.; Ebben, C. J.; Forestieri, S. D.; Guasco, T. L.; Hersey, S. P.; Kim, M. J.; Lambert, W. F.; Modini, R. L.; Mui, W.; Pedler, B. E.; Ruppel, M. J.; Ryder, O. S.; Schoepp, N. G.; Sullivan, R. C.; Zhao, D. Bringing the Ocean into the Laboratory to Probe the Chemical Complexity of Sea Spray Aerosol. *Proc. Natl. Acad. Sci. U.S.A.* **2013**, *110*, 7550–7555.
- (6) Rinaldi, M.; Fuzzi, S.; Decesari, S.; Marullo, S.; Santoleri, R.; Provenzale, A.; von Hardenberg, J.; Ceburnis, D.; Vaishya, A.; O'Dowd, C. D.; Facchini, M. C. Is Chlorophyll- a the Best Surrogate for Organic Matter Enrichment in Submicron Primary Marine Aerosol? *J. Geophys. Res.: Atmos.* 2013, 118, 4964–4973.
- (7) Patterson, J. P.; Collins, D. B.; Michaud, J. M.; Axson, J. L.; Sultana, C. M.; Moser, T.; Dommer, A. C.; Conner, J.; Grassian, V. H.; Stokes, M. D.; Deane, G. B.; Evans, J. E.; Burkart, M. D.; Prather, K. A.; Gianneschi, N. C. Sea Spray Aerosol Structure and Composition Using Cryogenic Transmission Electron Microscopy. *ACS Cent. Sci.* **2016**, *2*, 40–47.
- (8) Malfatti, F.; Lee, C.; Tinta, T.; Pendergraft, M. A.; Celussi, M.; Zhou, Y.; Sultana, C. M.; Rotter, A.; Axson, J. L.; Collins, D. B.; Santander, M. V.; Anides Morales, A. L.; Aluwihare, L. I.; Riemer, N.; Grassian, V. H.; Azam, F.; Prather, K. A. Detection of Active Microbial Enzymes in Nascent Sea Spray Aerosol: Implications for Atmospheric Chemistry and Climate. *Environ. Sci. Technol. Lett.* **2019**, *6*, 171–177.
- (9) Kasparian, J.; Hassler, C.; Ibelings, B.; Berti, N.; Bigorre, S.; Djambazova, V.; Gascon-Diez, E.; Giuliani, G.; Houlmann, R.; Kiselev, D.; De Laborie, P.; Le, A. D.; Magouroux, T.; Neri, T.; Palomino, D.; Pfändler, S.; Ray, N.; Sousa, G.; Staedler, D.; Tettamanti, F.; Wolf, J. P.; Beniston, M. Assessing the Dynamics of Organic Aerosols over the North Atlantic Ocean. *Sci. Rep.* **2017**, *7*, 45476.
- (10) Toprak, E.; Schnaiter, M. Fluorescent Biological Aerosol Particles Measured with the Waveband Integrated Bioaerosol Sensor WIBS-4: Laboratory Tests Combined with a One Year Field Study. *Atmos. Chem. Phys.* **2013**, *13*, 225–243.
- (11) Yue, S.; Ren, L.; Song, T.; Li, L.; Xie, Q.; Li, W.; Kang, M.; Zhao, W.; Wei, L.; Ren, H.; Sun, Y.; Wang, Z.; Ellam, R. M.; Liu, C. Q.; Kawamura, K.; Fu, P. Abundance and Diurnal Trends of Fluorescent Bioaerosols in the Troposphere over Mt. Tai, China, in Spring. J. Geophys. Res.: Atmos. 2019, 124, 4158–4173.
- (12) Photobiogeochemistry of Organic Matter; Mostofa, K. M. G., Yoshioka, T., Mottaleb, A., Vione, D., Eds.; Environmental Science and Engineering; Springer Berlin Heidelberg: Berlin, Heidelberg, 2013.
- (13) Zhang, Y.; Yin, Y.; Feng, L.; Zhu, G.; Shi, Z.; Liu, X.; Zhang, Y. Characterizing Chromophoric Dissolved Organic Matter in Lake Tianmuhu and Its Catchment Basin Using Excitation-Emission Matrix Fluorescence and Parallel Factor Analysis. *Water Res.* **2011**, *45*, 5110–5122.
- (14) Nebbioso, A.; Piccolo, A. Molecular Characterization of Dissolved Organic Matter (DOM): A Critical Review. *Anal. Bioanal. Chem.* **2013**, 405, 109–124.
- (15) Gabey, A. M.; Gallagher, M. W.; Whitehead, J.; Dorsey, J. R.; Kaye, P. H.; Stanley, W. R. Measurements and Comparison of Primary Biological Aerosol above and below a Tropical Forest Canopy Using a Dual Channel Fluorescence Spectrometer. *Atmos. Chem. Phys.* **2010**, *10*, 4453–4466.
- (16) Crawford, I.; Gallagher, M. W.; Bower, K. N.; Choularton, T. W.; Flynn, M. J.; Ruske, S.; Listowski, C.; Brough, N.; Lachlan-Cope, T.; Fleming, Z. L.; Foot, V. E.; Stanley, W. R. Real-Time Detection of Airborne Fluorescent Bioparticles in Antarctica. *Atmos. Chem. Phys.* **2017**, *17*, 14291–14307.
- (17) Savage, N. J.; Krentz, C. E.; Könemann, T.; Han, T. T.; Mainelis, G.; Pöhlker, C.; Huffman, J. A. Systematic Characterization and Fluorescence Threshold Strategies for the Wideband Integrated Bioaerosol Sensor (WIBS) Using Size-Resolved Biological and Interfering Particles. *Atmos. Meas. Tech.* **2017**, *10*, 4279–4302.

- (18) Hernandez, M.; Perring, A. E.; McCabe, K.; Kok, G.; Granger, G.; Baumgardner, D. Chamber Catalogues of Optical and Fluorescent Signatures Distinguish Bioaerosol Classes. *Atmos. Meas. Tech.* **2016**, *9*, 3283–3292.
- (19) Stokes, M. D.; Deane, G. B.; Prather, K.; Bertram, T. H.; Ruppel, M. J.; Ryder, O. S.; Brady, J. M.; Zhao, D. A Marine Aerosol Reference Tank System as a Breaking Wave Analogue for the Production of Foam and Sea-Spray Aerosols. *Atmos. Meas. Tech.* **2013**, *6*, 1085–1094.
- (20) Lee, C.; Sultana, C. M.; Collins, D. B.; Santander, M. V.; Axson, J. L.; Malfatti, F.; Cornwell, G. C.; Grandquist, J. R.; Deane, G. B.; Stokes, M. D.; Azam, F.; Grassian, V. H.; Prather, K. A. Advancing Model Systems for Fundamental Laboratory Studies of Sea Spray Aerosol Using the Microbial Loop. *J. Phys. Chem. A* **2015**, *119*, 8860–8870.
- (21) Stokes, M. D.; Deane, G.; Collins, D. B.; Cappa, C.; Bertram, T.; Dommer, A.; Schill, S.; Forestieri, S.; Survilo, M. A Miniature Marine Aerosol Reference Tank (MiniMART) as a Compact Breaking Wave Analogue. *Atmos. Meas. Tech.* **2016**, *9*, 4257–4267.
- (22) Collins, D. B.; Zhao, D. F.; Ruppel, M. J.; Laskina, O.; Grandquist, J. R.; Modini, R. L.; Stokes, M. D.; Russell, L. M.; Bertram, T. H.; Grassian, V. H.; Deane, G. B.; Prather, K. A. Direct Aerosol Chemical Composition Measurements to Evaluate the Physicochemical Differences between Controlled Sea Spray Aerosol Generation Schemes. *Atmos. Meas. Tech.* **2014**, *7*, 3667–3683.
- (23) Guillard, R. R. L.; Ryther, J. H. Studies of Marine Planktonic Diatoms: I. Cyclotella Nana Hustedt, and Detonula Confervacea (Cleve) Gran. Can. J. Microbiol. 1962, 8, 229–239.
- (24) Pöhlker, C.; Huffman, J. A.; Pöschl, U. Atmospheric Measurement Techniques Autofluorescence of Atmospheric Bioaerosols-Fluorescent Biomolecules and Potential Interferences. *Atmos. Meas. Tech.* **2012**, *5*, 37–71.
- (25) Lee, H. D.; Morris, H. S.; Laskina, O.; Sultana, C. M.; Lee, C.; Jayarathne, T.; Cox, J. L.; Wang, X.; Hasenecz, E. S.; Demott, P. J.; Bertram, T. H.; Cappa, C. D.; Stone, E. A.; Prather, K. A.; Grassian, V. H.; Tivanski, A. V. Organic Enrichment, Physical Phase State, and Surface Tension Depression of Nascent Core-Shell Sea Spray Aerosols during Two Phytoplankton Blooms. *ACS Earth Space Chem.* **2020**, *4*, 650–660.
- (26) Eiguren Fernandez, A.; Lewis, G. S.; Hering, S. V. Design and Laboratory Evaluation of a Sequential Spot Sampler for Time-Resolved Measurement of Airborne Particle Composition. *Aerosol Sci. Technol.* **2014**, *48*, 655–663.
- (27) Bidle, K. D.; Azam, F. Bacterial Control of Silicon Regeneration from Diatom Detritus: Significance of Bacterial Ectohydrolases and Species Identity. *Limnol. Oceanogr.* **2001**, *46*, 1606–1623.
- (28) Pedler, B. E.; Aluwihare, L. I.; Azam, F. Single Bacterial Strain Capable of Significant Contribution to Carbon Cycling in the Surface Ocean. *Proc. Natl. Acad. Sci. U.S.A.* **2014**, *111*, 7202–7207.
- (29) Azam, F.; Fenchel, T.; Field, J.; Gray, J.; Meyer-Reil, L.; Thingstad, F. The Ecological Role of Water-Column Microbes in the Sea. *Mar. Ecol.: Prog. Ser.* **1983**, *10*, 257–263.
- (30) Kaye, P. H.; Stanley, W. R.; Hirst, E.; Foot, E. V.; Baxter, K. L.; Barrington, S. J. Single Particle Multichannel Bio-Aerosol Fluorescence Sensor. *Opt. Express* **2005**, *13*, 3583–3593.
- (31) Gabey, A. M.; Stanley, W. R.; Gallagher, M. W.; Kaye, P. H. The Fluorescence Properties of Aerosol Larger than 0.8 Mm in Urban and Tropical Rainforest Locations. *Atmos. Chem. Phys.* **2011**, *11*, 5491–5504.
- (32) Forde, E.; Gallagher, M.; Walker, M.; Foot, V.; Attwood, A.; Granger, G.; Sarda-Estève, R.; Stanley, W.; Kaye, P.; Topping, D. Intercomparison of Multiple UV-LIF Spectrometers Using the Aerosol Challenge Simulator. *Atmosphere* **2019**, *10*, 797.
- (33) Robinson, E. S.; Gao, R.-S.; Schwarz, J. P.; Fahey, D. W.; Perring, A. E. Fluorescence Calibration Method for Single-Particle Aerosol Fluorescence Instruments. *Atmos. Meas. Tech.* **2017**, *10*, 1755–1768.

- (34) Kaye, P. H.; Aptowicz, K.; Chang, R. K.; Foot, V.; Videen, G. Angularly Resolved Elastic Scattering From Airborne Particles. *Optics of Biological Particles*; Springer Netherlands, 2007; pp 31–61.
- (35) Lawaetz, A. J.; Stedmon, C. A. Fluorescence Intensity Calibration Using the Raman Scatter Peak of Water. *Appl. Spectrosc.* **2009**, *63*, 936–940.
- (36) Murphy, K. R. Note on Determining the Extent of the Water Raman Peak in Fluorescence Spectroscopy. *Appl. Spectrosc.* **2011**, *65*, 233–236.
- (37) Coble, P. G. Characterization of Marine and Terrestrial DOM in Seawater Using Excitation-Emission Matrix Spectroscopy. *Mar. Chem.* **1996**, *51*, 325–346.
- (38) Determann, S.; Lobbes, J. M.; Reuter, R.; Rullkötter, J. Ultraviolet Fluorescence Excitation and Emission Spectroscopy of Marine Algae and Bacteria. *Mar. Chem.* 1998, 62, 137–156.
- (39) Lakowicz, J. R. Principles of Fluorescence Spectroscopy; Springer, 2006.
- (40) Hessen, D. O.; Tranvik, L. J. Aquatic Humic Substances: Ecology and Biochemistry; Springer-Verlag Berlin Heidelberg: Berlin, 1998; Vol. 133.
- (41) Liu, L.; Huang, Q.; Zhang, Y.; Qin, B.; Zhu, G. Excitation-Emission Matrix Fluorescence and Parallel Factor Analyses of the Effects of N and P Nutrients on the Extracellular Polymeric Substances of Microcystis Aeruginosa. *Limnologica* **2017**, *63*, 18–26.
- (42) Fennelly, M.; Sewell, G.; Prentice, M.; O'Connor, D.; Sodeau, J. Review: The Use of Real-Time Fluorescence Instrumentation to Monitor Ambient Primary Biological Aerosol Particles (PBAP). *Atmosphere* **2018**, *9*, 39.
- (43) Rastelli, E.; Corinaldesi, C.; Dell'anno, A.; Lo Martire, M.; Greco, S.; Cristina Facchini, M.; Rinaldi, M.; O'Dowd, C.; Ceburnis, D.; Danovaro, R. Transfer of Labile Organic Matter and Microbes from the Ocean Surface to the Marine Aerosol: An Experimental Approach. *Sci. Rep.* **2017**, *7*, 11475.
- (44) Shaffer, B. T.; Lighthart, B. Survey of Culturable Airborne Bacteria at Four Diverse Locations in Oregon: Urban, Rural, Forest, and Coastal. *Microb. Ecol.* **1997**, *34*, 167–177.
- (45) Mari, X.; Kiørboe, T. Abundance, Size Distribution and Bacterial Colonization of Transparent Exopolymeric Particles (TEP) during Spring in the Kattegat. *J. Plankton Res.* **1996**, *18*, 969–986.
- (46) Aller, J. Y.; Kuznetsova, M. R.; Jahns, C. J.; Kemp, P. F. The Sea Surface Microlayer as a Source of Viral and Bacterial Enrichment in Marine Aerosols. *J. Aerosol Sci.* **2005**, *36*, 801–812.
- (47) Smith, D. C.; Simon, M.; Alldredge, A. L.; Azam, F. Intense Hydrolytic Enzyme Activity on Marine Aggregates and Implications for Rapid Particle Dissolution. *Nature* **1992**, 359, 139–142.
- (48) Grzybowski, W. Selected Properties of Different Molecular Size Fractions of Humic Substances Isolated from Surface Baltic Water in the Gdańsk Deep Area. *Oceanologia* **1996**, *38*, 33–47.
- (49) Benner, R.; Pakulski, J. D.; McCarthy, M.; Hedges, J. I.; Hatcher, P. G. Bulk Chemical Characteristics of Dissolved Organic Matter in the Ocean. *Science* **1992**, *255*, 1561–1564.
- (50) Andersson, M.; Catalán, N.; Rahman, Z.; Tranvik, L.; Lindström, E. Effects of Sterilization on Dissolved Organic Carbon (DOC) Composition and Bacterial Utilization of DOC from Lakes. *Aquat. Microb. Ecol.* **2018**, *82*, 199–208.
- (51) Gantt, B.; Meskhidze, N. The Physical and Chemical Characteristics of Marine Primary Organic Aerosol: A Review. *Atmos. Chem. Phys.* **2013**, *13*, 3979–3996.
- (52) Burrows, S. M.; Hoose, C.; Pöschl, U.; Lawrence, M. G. Ice Nuclei in Marine Air: Biogenic Particles or Dust? *Atmos. Chem. Phys.* **2013**, *13*, 245–267.
- (53) Vergara-Temprado, J.; Murray, B. J.; Wilson, T. W.; O'Sullivan, D.; Browse, J.; Pringle, K. J.; Ardon-Dryer, K.; Bertram, A. K.; Burrows, S. M.; Ceburnis, D.; Demott, P. J.; Mason, R. H.; O'Dowd, C. D.; Rinaldi, M.; Carslaw, K. S. Contribution of Feldspar and Marine Organic Aerosols to Global Ice Nucleating Particle Concentrations. *Atmos. Chem. Phys.* **2017**, *17*, 3637–3658.

(54) Andreae, M. O.; Rosenfeld, D. Aerosol-Cloud-Precipitation Interactions. Part 1. The Nature and Sources of Cloud-Active Aerosols. *Earth-Sci. Rev.* **2008**, *89*, 13–41.